

The Stochastic Perturbation – Based Finite Volume Method for 1 & 2D Fluid and Heat Flow Problems

Marcin KAMIŃSKI

*Department of Steel Structures, Technical University of Łódź
Al. Politechniki 6, 90–924 Łódź, POLAND*

Rafał L. OSSOWSKI

*PhD student, Faculty of Civil Engineering,
Architecture and Environmental Engineering
Technical University of Łódź
Al. Politechniki 6, 90–924 Łódź, POLAND*

Received (17 March 2010)

Revised (20 April 2010)

Accepted (18 May 2010)

This article is devoted to the mathematical formulation and computational implementation of the Stochastic Finite Volume Method for 1 and 2D fluid and heat flow problems. It is based on the stochastic generalized perturbation technique, which allows for a determination of the probabilistic moments of the state variables or functions for the general stationary transport equations with random parameters. Both numerical case studies contain a comparison of the stochastic perturbation approach of different orders, their relations to the Monte–Carlo simulation results as well as the effect of the perturbation parameter and input coefficient of variation on the output state functions.

Keywords: Finite Volume Method, stochastic perturbation technique, the response function method, Monte–Carlo simulation, convection–diffusion problems, symbolic computing

1. Introduction

The flow (or transport) problems with random physical coefficients and/or geometrical parameters appear frequently in the engineering practice. From a probabilistic point of view they can be solved using the Monte–Carlo simulation technique as well as the stochastic methods based on the Karhunen-Loeve or polynomial expansions [5, 10] or the Taylor expansion perturbation technique [6, 7, 8]. On the other hand, whether a spatial discretization of the transport equations in solids seems to be more natural using the Finite Element Method (FEM), then a the fluid or aero-mechanics applications need rather volumes–based than the specific points of continuum discretization. Therefore, the Finite Volume Method (FVM) [1, 3, 4]

seems to be more appropriate in the last two case studies.

That is why this elaboration is entirely devoted to probabilistic formulation of the FVM approach using the generalized perturbation technique. This generalization is expressed by an inclusion in the model equations both perturbation parameter ε as well as the probabilistic moments of the random input of practically any available order. Therefore, any order probabilistic moments of the stochastic output can be computed and although the Gaussian random variables are analyzed here, then any type of the probability density function may be effectively taken instead of it. The details of computational implementation of the stochastic perturbation-based approach into the classical FVM are given here independently for the unidirectional (diffusion-advection) and planar (heat conduction) problems. The numerical routines built up allows to compute any probabilistic moments and the coefficients for the state functions analyzed by (a) straightforward differentiation of an increasing order equations systems within the perturbation scheme and (b) the use of the so-called response function method. Alternatively, we may determine the same by the classical Monte-Carlo simulation technique embedded symbolically into the MAPLE flow solvers here. All the numerical results provided here show efficiently that neglecting a choice between the methods (a) and (b), the SFVM gives the results (for higher order realizations) almost the same as the statistical estimation obtained thanks to the Monte-Carlo analysis.

Although a computational implementation is completed here using the symbolic language of the system MAPLE, further programming of the general purpose SFVM program seems to be the relatively easy task, which can give a plenty of new interesting and reliable results. So that, the new problems like 1D, 3D and even planar using the other grids (both structured and unstructured) for uncoupled and coupled physical phenomena with random coefficients should be studied using the presented technique. The very important reason to develop this method is a discretization of the input random fields by the SFVM, which seems to be easier than in the case of the Stochastic Finite and Boundary Element Methods. Since the center of each sub-volume is equivalent to its degree-of-freedom location, this particular point is further considered to compute the cross-correlation matrices for higher order moments and random fields analysis. An analogous process is much more complex for both SFEM, because usually the mid-point discretization is employed for the random fields in 2 and 3D problems. Those points are however not equivalent to the degrees of freedom locations, so that quite separate computations are needed to determine the probabilistic moments. Local high gradients of the cross-correlations may essentially affect the error of the correlations determination for the state functions in the SFEM, whereas the SFVM is free from this effect since spatial and random fields discretizations are done on the same subsets of computational domain.

2. The Finite Volume Method

As it is known, the Finite Volume Method (FVM) is one of the available computer methods for evaluation of the partial differential equations as a system of the algebraic equations. A very useful property of the FVM is that the balance principles, which are the basis for the mathematical modeling of continuum mechanical prob-

lems, per definition, are also fulfilled for the discrete equations. A starting point for the FVM is a decomposition of the problem domain into the control volumes (CVs), where each CV is represented by its midpoint only. This is the main difference to the Finite Element Method (FEM), where the equilibrium equations are formed and solved in the nodal points of the mesh only, which are located on the corners (and midpoints for higher order approximants) of each finite element. Let us note that, quite similarly to the FEM, there are (a) regular and irregular point of the grid, quite similar to those applied in the Finite Difference Methods, (b) triangular, quadrilateral as well as the polygonal grids, both structured and unstructured in plane FVM discretizations as well as (c) some volumetric divisions using cubes, for instance, where the gravity center of such a cube may be treated as the point of the FVM grid.

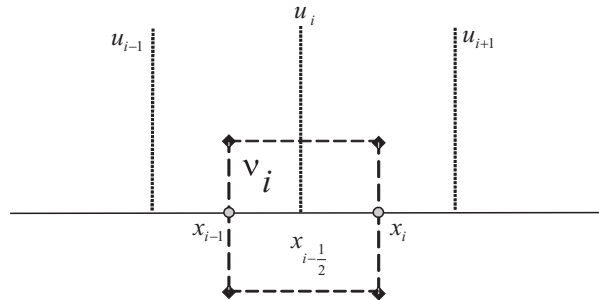


Figure 1 Cell – centered FVM

2.1. 1D example for the convection–diffusion equation

Let us consider the one dimension flow described by transport equation with boundary value:

$$\begin{aligned}
 \nu \frac{\partial u}{\partial x} - d \frac{\partial^2 u}{\partial x^2} &= 0 \text{ in } (0, 1) \\
 u(0) &= 0 \\
 u(1) &= 1
 \end{aligned}
 \tag{1}$$

ν is constant flow velocity (in a subsonic flow regime), u is a displacement of the fluid in the horizontal direction and d stands for the diffusion coefficient, which is the physical parameter; let us note that $\nu > 0$. We provide a discretization by division of the computational domain V onto the non-overlapping control volumes $V_i, i=1, \dots, n$.

$$V = \sum_{i=1}^n V_i \quad i, n \in \mathbb{N}, \quad V \in \mathbb{R}
 \tag{2}$$

Next, it is necessary to discretize eqn (1) using chosen type of approximation (UDS – upwind difference scheme, CDS – central difference scheme or one of most advanced – LUDS – linear upwind difference scheme and QUICK – quadratic upwind difference scheme) by using only local information for all control volumes. Obviously, the FVM method is universal and can be used for different state variables (i.e. u , v , T), while the UDS approximation of the convective fluxes is represented by the following formula:

$$I_c \approx \nu \frac{u_i - u_{i-1}}{\Delta x}, \quad \text{for } \nu > 0 \quad u_{i-\frac{1}{2}} \approx u_{i-1}, \quad u_{i+\frac{1}{2}} \approx u_i, \quad i = 1, \dots, n \quad (3)$$

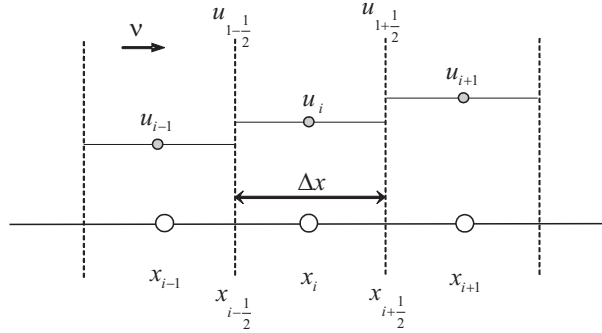


Figure 2 1D upwind difference approximation (UDS)

The diffusive fluxes are approximated here in the same way. There holds

$$\left(\frac{\partial u}{\partial x} \right)_{i-\frac{1}{2}} \approx \frac{u_i - u_{i-1}}{\Delta x}, \quad \left(\frac{\partial u}{\partial x} \right)_{i+\frac{1}{2}} \approx \frac{u_{i+1} - u_i}{\Delta x} \quad (4)$$

and the second-order accurate central difference is given by

$$I_d \approx -d \frac{u_{i-1} - 2u_i + u_{i+1}}{(\Delta x)^2} \quad (5)$$

The upwind difference scheme gives the linear system of equations, which can be finally written as

$$Pe \frac{u_i - u_{i-1}}{\Delta x} - \frac{u_{i-1} - 2u_i + u_{i+1}}{(\Delta x)^2} = 0 \quad i = 1, \dots, N-1 \quad (6)$$

where $Pe = \frac{\nu}{d}$ is the Peclet number. Therefore, a matrix formulation for the FVM can be rewritten using the constant coefficients a , b and c as follows

$$A = \frac{1}{(\Delta x)^2} \begin{bmatrix} b & c & & & \\ a & b & c & & \\ & a & b & c & \\ & & \cdot & \cdot & \cdot \\ & & & a & b \end{bmatrix} \quad u = \begin{bmatrix} u_1 \\ u_2 \\ u_3 \\ \cdot \\ u_{N-1} \end{bmatrix} \quad F = \begin{bmatrix} 0 \\ 0 \\ 0 \\ \cdot \\ -\frac{c}{(\Delta x)^2} \end{bmatrix} \quad (7)$$

where

$$a = -1 - Pe\Delta x, \quad b = 2 + Pe\Delta x, \quad c = -1$$

So that the discretization is uniform here (but it needn't be) and Δx naturally affects the final solution quality.

2.2. Plane heat conduction problem by the FVM

The introduced control volume refers, in our case, to a small plate (the specific example included here contains the quadrilateral CV with a cell-oriented arrangement of nodes Fig. 1) surrounding each node point on a mesh.

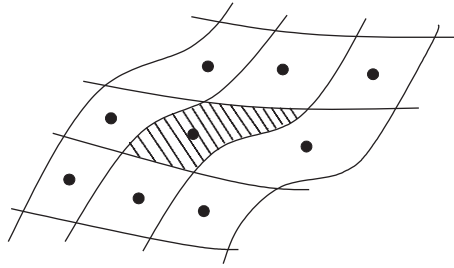


Figure 3 Cell-oriented control volumes

The next step is a formulation of the integral balance equation within each control volume and approximation of the surface and volume integrals by the relevant numerical integration. Last step is formulation and solving algebraic system of equations with the concrete boundary conditions. We consider here the heat conduction in a trapezoidal plate described by the heat conduction equation with the homogeneous boundary conditions as indicated in Fig. 3 [7, 9]

$$\begin{aligned} -k \left(\frac{\partial^2 T}{\partial x^2} + \frac{\partial^2 T}{\partial y^2} \right) &= \rho q \\ T &= \hat{T}, \quad x \in \partial\Omega_T \\ q &= \hat{q}, \quad x \in \partial\Omega_q \end{aligned} \quad (8)$$

Let us consider statistically homogeneous region with constant material density, heat conductivity (random quantity) as well as the constant heat source applied all onto the plate. An integration of eqn (8) over a control volume V according to the Gauss integral theorem and assuming that the surface integral may be splitted into a sum of the four surface integrals over the cell faces S_c of the CV gives [9]

$$-k \sum_c \int_{S_c} \left(\frac{\partial T}{\partial x} n_x + \frac{\partial T}{\partial y} n_y \right) dS_c = \int_V \rho q dV = \rho \sum_c F_c \quad (9)$$

where a summation is carried out over $c = e, w, n, s$ according to the so-called compass notation, which is useful for quadrilateral control volume.

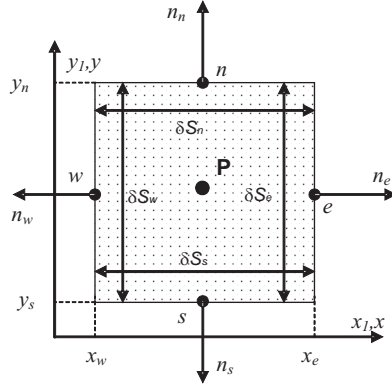


Figure 4 The quadrangular control volume with so-called compass notations in the Cartesian grids

Generally, the balance equations describing the stationary transport problem has the form:

$$\frac{\partial}{\partial x_i} \left(\rho v_i \phi - \alpha \frac{\partial \phi}{\partial x_i} \right) = f \quad (10)$$

where α is the scalar field coefficient equivalent to the heat conductivity in steady-state heat transfer.

By integration of (10) over an arbitrary control volume V and application of the Gauss integral theorem our equation has form:

$$\int_S \left(\rho v_i \phi - \alpha \frac{\partial \phi}{\partial x_i} \right) n_i dS = \int_V f dV \quad (11)$$

The surface integral in (11) can be changed into the sum according to the formula:

$$\sum_c \int_{S_c} \left(\rho v_i \phi - \alpha \frac{\partial \phi}{\partial x_i} \right) n_{ci} dS_c = \int_V f dV, \quad \text{where } c = 1, \dots, k \quad (12)$$

where c represents all surfaces over the cell faces of the CV's.

Using the midpoint rule for the surface integrals and distinguishing between the convective and diffusive part of equations (splitting of the convective and diffusive fluxes),

$$F_c^{convective} = \int_{S_c} \rho v_i \phi n_{ci} dS_c \quad \text{and} \quad F_c^{diffusive} = - \int_{S_c} \left(\alpha \frac{\partial \phi}{\partial x_i} \right) n_{ci} dS_c \quad (13)$$

Considering homogenous medium it is easy to see, that:

$$\int_{S_c} \rho v_i \phi n_{ci} dS_c = \rho \sum_{i=1}^n v_i \phi n_{ci} d(\partial\Omega) \quad (14)$$

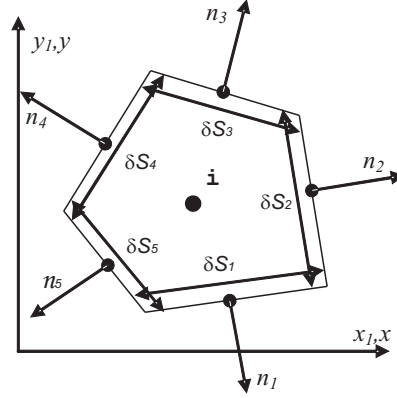


Figure 5 Control volume with general notations in the Cartesian grids

where n denotes the total number of control volumes and

$$-\int_{S_c} \left(\alpha \frac{\partial \phi}{\partial x_i} \right) n_{ci} dS_c = \alpha \sum_{i=1}^m n_{ci} \left(\frac{\partial \phi}{\partial x_i} \right)_c d(\partial \Omega) \quad (15)$$

where m denotes the total number of separate lines constituting the considered control polygonal. Returning to the compass notation we obtain the approximations:

$$\sum_c \rho v_i n_{ci} \delta S_c \phi_c - \sum_c \alpha n_{ci} \delta S_c \left(\frac{\partial \phi}{\partial x_i} \right)_c = f_P \delta V \quad (16)$$

convective part of equation diffusive part of equation

Where:

$$n_e = \frac{(y_{ne} - y_{se})}{\delta S_e} e_1 - \frac{(x_{ne} - x_{se})}{\delta S_e} e_2 \quad (17)$$

and

$$\delta S_e = \sqrt{(x_{ne} - x_{se})^2 + (y_{ne} - y_{se})^2} \quad (18)$$

Approximation of the volume integral in the CV are represented by average value over the CV according to two-dimensional midpoint rule:

$$\int_V \rho_i q_i dV = \int_V f_i dV \approx f_P \delta V \quad (19)$$

where δV denotes the volume of the CV and f_i denotes the value of the function f .

$$\delta V = \frac{1}{2} |(x_{se} - x_{nw})(y_{ne} - y_{sw}) - (x_{ne} - x_{sw})(y_{se} - y_{nw})| \quad (20)$$

Difference formulas can be simply approximate by using central differencing formula.

$$\left(\frac{\partial\phi}{\partial x}\right)_e \approx \frac{\phi_E - \phi_P}{x_E - x_P} \quad (21)$$

Where ϕ is a linear function between the points x_P and x_E .

For the velocity components $v_1, v_2 > 0$ and using the *UDS* method for the convective flux, and the *CDS* method for diffusive flux the balance equation (16) for the P'th node can be written:

$$\begin{aligned} & \left(\rho v_1 \phi_P - \alpha \frac{\phi_E - \phi_P}{x_E - x_P}\right)(y_n - y_s) - \left(\rho v_1 \phi_W - \alpha \frac{\phi_P - \phi_W}{x_P - x_W}\right)(y_n - y_s) \\ & + \left(\rho v_2 \phi_P - \alpha \frac{\phi_N - \phi_P}{y_N - y_P}\right)(x_e - x_w) - \left(\rho v_2 \phi_S - \alpha \frac{\phi_P - \phi_S}{y_P - y_S}\right)(x_e - x_w) \\ & = f_P (y_n - y_s)(x_e - x_w) \end{aligned} \quad (22)$$

Small reorganizations gives as an algebraic equation:

$$a_P \phi_P = a_E \phi_E + a_W \phi_W + a_N \phi_N + a_S \phi_S + f_P \quad (23)$$

with coefficients:

$$\begin{aligned} a_P &= \frac{\rho v_1}{x_e - x_w} + \frac{\alpha(x_E - x_W)}{(x_P - x_W)(x_E - x_P)(x_e - x_w)} + \frac{\rho v_2}{y_n - y_s} \\ &+ \frac{\alpha(y_N - y_S)}{(y_P - y_S)(y_N - y_P)(y_n - y_s)} \\ a_E &= \frac{\alpha}{(x_E - x_P)(x_e - x_w)} \\ a_W &= \frac{\rho v_1}{x_e - x_w} + \frac{\alpha}{(x_P - x_W)(x_e - x_w)} \\ a_N &= \frac{\alpha}{(y_N - y_P)(y_n - y_s)} \quad a_S = \frac{\rho v_2}{y_n - y_s} + \frac{\alpha}{(y_P - y_S)(y_n - y_s)} \end{aligned} \quad (24)$$

which generally can be written as:

$$a_P \phi_P - \sum_c a_c \phi_c = f_P \quad (25)$$

In particular 2D case described by the equation (9), algebraic equations in the context of temperatures are given as follows:

$$k_P^{[i,j]} T_P^{[i,j]} - k_E^{[i,j]} T_E^{[i,j]} - k_W^{[i,j]} T_W^{[i,j]} - k_S^{[i,j]} T_S^{[i,j]} - k_N^{[i,j]} T_N^{[i,j]} = f_P^{[i,j]} \quad (26)$$

where $i = 1, \dots, M, j = 1, \dots, N$.

where T_α is the vector of unknown temperatures – the solution vector, $K_{\alpha\beta}$ is the matrix of the heat conductivity, F_α is the vector of applied heat fluxes and α, β indexing all available degrees of freedom within the control volumes; N denotes here the number of the control volumes introduced in the computational domain.

A contradiction of 1 and 2D FVM discretizations shows that the unidirectional one is closer to the Finite Difference Method like division of a computational domain (because of its difference form), whereas 2D (as well as 3D not shown here) is closer to the Finite Element Method discretization because the weak form of the problem is subdivided into the control volumes.

3. The Perturbation – based Stochastic Finite Volume Method

Let us denote the corresponding random vector of the problem by b , with probability density functions $p(b)$. Therefore, the m^{th} order central probabilistic moment is given by

$$\mu_m(b) = \int_{-\infty}^{+\infty} (b - E[b])^m p(b) db \quad (29)$$

The basic idea of the stochastic perturbation approach follows the classical perturbation expansion idea and is based on approximation of all input variables and the state functions of the problem via the truncated Taylor series about their spatial expectations in terms of a parameter $\varepsilon > 0$. For example, in the case of the heat conductivity k , the n^{th} order truncated expressions are written as

$$k = k^0 + \varepsilon k^{,b} \Delta b + \frac{1}{2} \varepsilon^2 k^{,bb} \Delta b \Delta b + \dots + \frac{1}{n!} \varepsilon^n k^{(n)} (\Delta b)^n \quad (30)$$

where

$$\varepsilon \Delta b = \varepsilon (b - b^0) \quad (31)$$

is the first variation of b about its expected value b^0 and, similarly

$$\varepsilon^2 \Delta b \Delta b = \varepsilon^2 (b - b^0) (b - b^0) \quad (32)$$

is the second variation of b about b^0 ; the n th order variation can be expressed analogously as

$$\varepsilon^n (\Delta b)^n = \varepsilon^n (b - b^0)^n \quad (33)$$

The symbol $(\cdot)^0$ represents the value of the function (\cdot) taken at the expectations b^0 , while $(\cdot)^b$, $(\cdot)^{bb}$ and $(\cdot)^{(n)}$ denote the first, the second and n th order partial derivatives. The fluid velocity may be expanded as

$$\nu_i = \nu_i^0 + \varepsilon \nu_i^{,b} \Delta b + \frac{1}{2} \varepsilon^2 \nu_i^{,bb} \Delta b \Delta b + \dots + \frac{1}{n!} \varepsilon^n \nu_i^{(n)} (\Delta b)^n \quad (34)$$

Traditionally, the stochastic perturbation approach to all the physical problems is entered by the respective perturbed equations of the 0^{th} , 1^{st} and successively higher orders being a modification of the relevant variational integral formulation. It is well known from the SFEM formulations that the system of linear algebraic equations, which is the basis of the model, i.e.

$$K_{\alpha\beta}(b) T_\beta(b) = Q_\alpha(b), \quad \alpha, \beta = 1, \dots, N \quad (35)$$

where is the heat conductivity matrix, denotes the discrete temperatures vector in the system, while is the heat flux, may be transformed into the following systems of equations:

$$\begin{cases} K_{\alpha\beta}^0 T_{\beta}^0 = Q_{\alpha}^0 \\ K_{\alpha\beta}^0 T_{\beta}^b = Q_{\alpha}^b - K_{\alpha\beta}^b T_{\beta}^0 \\ (\dots) \\ \sum_{k=0}^n \binom{n}{k} K_{\alpha\beta}^{(k)} T_{\beta}^{(n-k)} = Q_{\alpha}^{(n)} \end{cases} \quad (36)$$

In order to calculate the expected values and higher order probabilistic moments of displacements, strains and stresses functions, the same Taylor expansion is employed to the definitions of probabilistic moments calculated for any state random variables assuming their continuous character. Therefore, the most important first two probabilistic moments of these functions are derived from the definition; it is explained below for the temperature history $T(b; t)$. The expectation equals to

$$\begin{aligned} E [T(t, b) ; b] &= \int_{-\infty}^{+\infty} T(t) p(b) db \\ &= \int_{-\infty}^{+\infty} \left(T^0 + \varepsilon T^{,b} \Delta b + \frac{1}{2} \varepsilon^2 T^{,bb} \Delta b \Delta b + \dots + \frac{1}{n!} \varepsilon^n T^{,n} (\Delta b)^n \right) p(b) db \end{aligned} \quad (37)$$

so that, the 6th order expansion reduces to

$$\begin{aligned} E [T(t, b) ; b] &\cong 1 \times T^0(t, b) + \frac{1}{2} \times T^{,bb}(t, b) \times Var(b) \\ &+ \frac{1}{4!} \times T^{,bbbb}(t, b) \times \mu_4(b) + \frac{1}{6!} \times T^{,bbbbbb}(t, b) \times \mu_6(b) \\ &= T^0(t, b) + \frac{1}{2} T^{(2)}(t, b) + \frac{1}{4!} T^{(4)}(t, b) + \frac{1}{6!} T^{(6)}(t, b) \end{aligned} \quad (38)$$

where the odd order terms are equal to zero for the Gaussian random deviates. In the case of a single Gaussian input random variable b , the generalized expansion simplifies of course to

$$\begin{aligned} E [T(t, b) ; b, \varepsilon, m] &= T^0(t, b) + \frac{1}{2} \varepsilon^2 \frac{\partial^2 T}{\partial b^2} \mu_2(b) \\ &+ \frac{1}{4!} \varepsilon^4 \frac{\partial^4 T}{\partial b^4} \mu_4(b) + \frac{1}{6!} \varepsilon^6 \frac{\partial^6 T}{\partial b^6} \mu_6(b) \\ &+ \dots + \frac{1}{(2m)!} \varepsilon^{2m} \frac{\partial^{2m} T}{\partial b^{2m}} \mu_{2m}(b) \end{aligned} \quad (39)$$

with μ_{2m} being the central $2m^{th}$ probabilistic moment. Considering that for a standard deviations denoted by σ

$$\mu_{2k+1}(b) = 0 \quad \mu_{2k}(b) = 1 \times 3 \times \dots \times (2k-1) \sigma^{2k}(b) \quad \text{for any } k \leq m \quad (40)$$

one may demonstrate that

$$\begin{aligned}\mu_2(b) &= \sigma^2(b) = Var(b) \\ \mu_4(b) &= 3\sigma^4(b) = 3Var^2(b) \\ \mu_6(b) &= 15\sigma^6(b) = 15Var^3(b)\end{aligned}\quad (41)$$

Using this extension of the random output, a desired efficiency of the expected values can be achieved by the appropriate choice of m and ε corresponding to the input probability density function (PDF) type, probabilistic moment interrelations, acceptable error of the computations, etc.; this choice can be made by comparative studies with Monte–Carlo simulations or theoretical results obtained by direct symbolic integration.

Quite a similar treatment to that from above leads to the following result for the variance of any state function; there holds

$$\begin{aligned}Var(T) &= (T^{,b})^2 \times \mu_2(b) + \left(\frac{1}{4} (T^{,bb})^2 + \frac{2}{3!} T^{,b} T^{,bbb} \right) \times \mu_4(b) \\ &+ \left(\left(\frac{1}{3!} \right)^2 (T^{,bbb})^2 + \frac{1}{4!} T^{,bbbb} T^{,bb} + \frac{2}{5!} T^{,bbbbb} T^{,b} \right) \times \mu_6(b)\end{aligned}\quad (42)$$

Consequently, m^{th} order probabilistic moment for the structural response function in the 10^{th} order stochastic Taylor expansion is introduced as

$$\begin{aligned}\mu_m(T(b)) &= \int_{-\infty}^{+\infty} \left(\sum_{i=1}^n \frac{\varepsilon^i}{i!} \Delta b^i \frac{\partial^i T}{\partial b^i} - E[T(b)] \right)^m p(b) db \\ &= \int_{-\infty}^{+\infty} \left(T^0(b) + T^{,b} \varepsilon \Delta b + T^{,bb} \varepsilon^2 \frac{(\Delta b)^2}{2!} \dots \frac{\partial^n T(b)}{\partial b^n} \varepsilon^n \frac{(\Delta b)^n}{n!} - E[T(b)] \right)^m p(b) db \\ &\cong \int_{-\infty}^{+\infty} \left(T^{,b} \varepsilon \Delta b + T^{,bb} \varepsilon^2 \frac{(\Delta b)^2}{2!} \dots \frac{\partial^{10} T(b)}{\partial b^{10}} \varepsilon^{10} \frac{(\Delta b)^{10}}{10!} \right)^m p(b) db\end{aligned}\quad (43)$$

It is necessary to point out that this methodology is valid for a single random variable with any probability density function; further simplifications may be obtained by a specification of this PDF. This methodology will be essentially changed in the case of random field as well as of two and more correlated random variables.

Now, the remaining numerical issue is a determination of the partial derivatives (and their stability) of the state functions with respect to the random input variable. The straightforward manner following eqns. (36), where $k + 1^{st}$ derivative is deduced from k^{th} order equation is not the only one. Let us introduce the n^{th} order polynomial representation of the state function T with respect to random input parameter b as

$$T(b) = a_n b^{n-1} + a_{n-1} b^{n-2} + \dots + a_0 \quad \text{where } a_n, \dots, a_0 \in \mathfrak{R} \quad (44)$$

Computational determination of those coefficients needs a formation and a solution of linear system of equations of the n^{th} order, which would be a result of the

repeated deterministic solution (35) within the new domain $[b - \Delta b, b + \Delta b]$, where the interval $2\Delta b$ is uniformly divided into $n - 1$ equidistant sub-domains. If the entire initial domain is statistically homogeneous with respect to the parameter b , then this extra system must be solved only once and the polynomial approximation (44) has a global character. Then, we solve numerically

$$K_{\alpha\beta}(b_i)T_{\beta}^{(i)}(b_i) = Q_{\alpha}(b_i), \quad i = 1, \dots, n, \quad \alpha, \quad \beta = 1, \dots, N \quad (45)$$

with respect to $T_{\beta}^{(i)}(b_i)$ and then the coefficients a_i are found as β -independent. The unique solution for this system makes it possible calculation of up to n^{th} order ordinary derivatives of the function T with respect to b as

- 1st order derivative

$$\frac{dT}{db} = (n - 1) a_1 b^{n-2} + (n - 2) a_2 b^{n-3} + \dots + a_{n-1} \quad (46)$$

- 2nd order derivative

$$\frac{d^2T}{db^2} = (n - 1)(n - 2) a_1 b^{n-3} + (n - 2)(n - 3) a_2 b^{n-4} + \dots + a_{n-2} \quad (47)$$

- kth order derivative

$$\frac{d^k T}{db^k} = \prod_{i=1}^k (n - i) a_1 b^{n-k} + \prod_{i=2}^k (n - i) a_2 b^{n-(k+1)} + \dots + a_{n-k} \quad (48)$$

Providing that the response function for $T(b)$ has a single independent argument being the input random variable of the problem, it is possible to employ the stochastic perturbation technique based on the Taylor representation to compute up to m^{th} order probabilistic moments. Including the above formulas for the derivatives of the response function into definition of probabilistic moments one can determine the expectations, variances as well as any order random characteristics.

4. Computational analysis

4.1. 1D flow computations

Computational analysis deals here with a determination of the probabilistic velocity profile by the Stochastic Finite Volume Methods for the computational domain presented in Fig. 3 below.

The channel height is divided into 10 control volumes with the constant length $\Delta x = 0.1$, the coefficient of variation for the diffusion coefficient is taken as 0.15, while its expected value results from the Peclet number adopted in this study as $Pe = 40$.

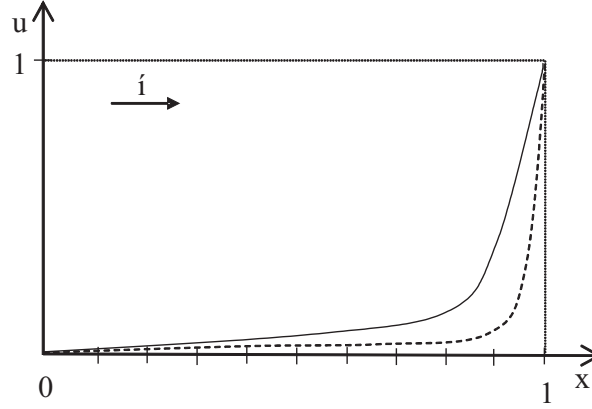


Figure 7 Discretization and the boundary conditions for the 1D flow case

Of the results is given in Figs 8-11, where the first figure shows a comparison of the deterministic upwind solution (expanded further towards the stochastic method) with the analytical profile. It is clear from this comparison that the upwind technique needs some further modifications to achieve more satisfactory accuracy. Figs 9, 10 and 11 contain consecutively the profiles of the variances, standard deviations as well as the third and fourth probabilistic moments of the function u . First two profiles are completed according to the 2nd, 4th and 6th order approaches, while higher than the second moments are derived from the first, the lowest order term within the corresponding expansions. It is clear from Fig. 9 and 10 that the probabilistic convergence for $\alpha(d) = 0.15$ is very fast since no differences between the profiles obtained for various perturbation orders are observed. Let us note also that the computations for the 4th central moments of the profile studied need larger expansion because of the numerical discrepancies determined within the second last subvolume, where (which cannot be justified theoretically at all).

4.2. 2D flow analysis

The entire computational part has been prepared and optimized in the MAPLE symbolic environment, versions 10 and 11, using the internal statistics and linear algebra options. This code is tested on the example of 2 finite volume discretisation of the heat transfer in trapezoidal plate (Fig. 12) with constant source of heat, material density [9] and heat conductivity k as the Gaussian random quantity with given first two probabilistic moments.

An approximation of the integrals by the midpoint rule and the derivatives at CV faces by second-order central differences gives an algebraic system of equations. There holds

$$F_e \approx -\frac{17}{9}(T_E - T_P) - 10 \quad F_w = 60 \quad F_s \approx 6T_P \quad F_n \approx 3T_P - 60 \quad (49)$$

for CV₁ and

$$F_e = 0 \quad F_w \approx \frac{17}{9}(T_P - T_W) + 10 \quad F_s \approx 6T_P \quad F_n \approx 3T_P - 60 \quad (50)$$

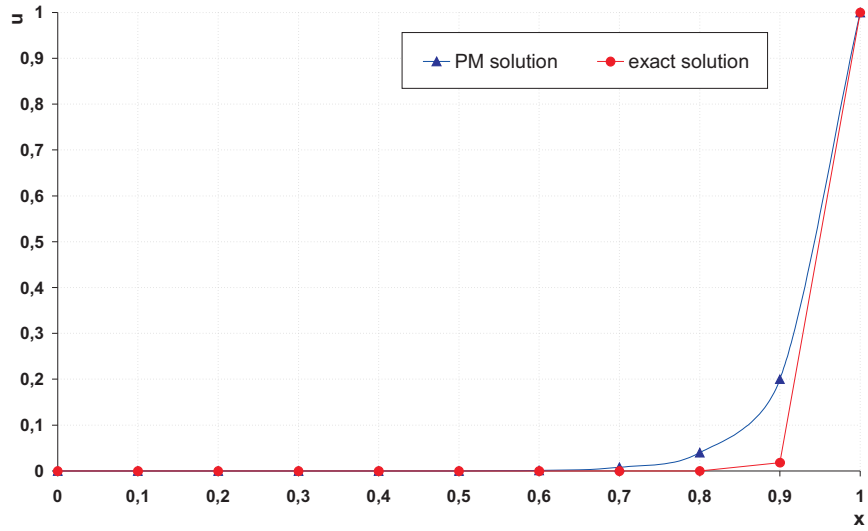


Figure 8 Comparison of the upwind technique against the theoretical results

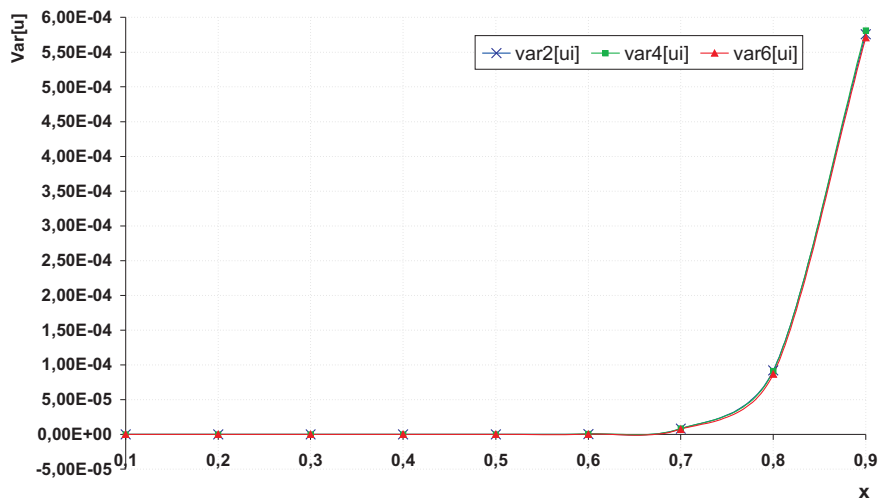


Figure 9 The variances of the fluid velocity as a function of the vertical coordinate

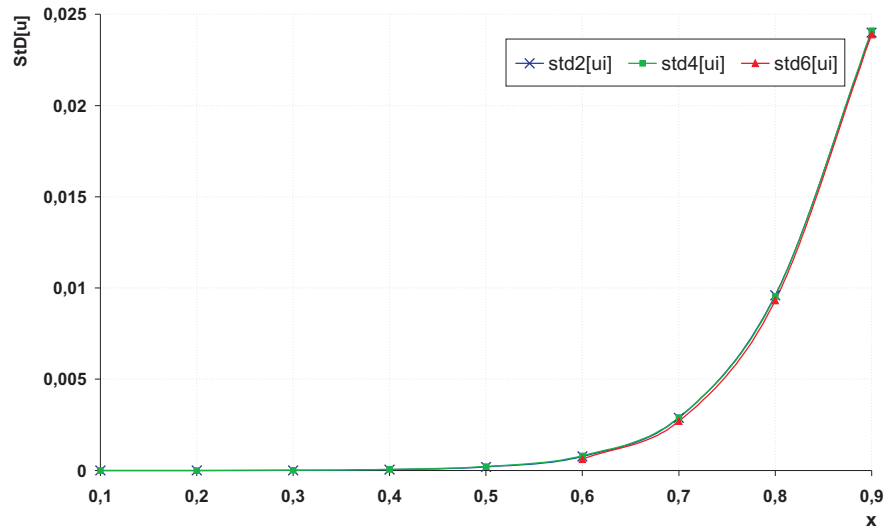


Figure 10 Standard deviations of the fluid velocity as a function of the vertical coordinate

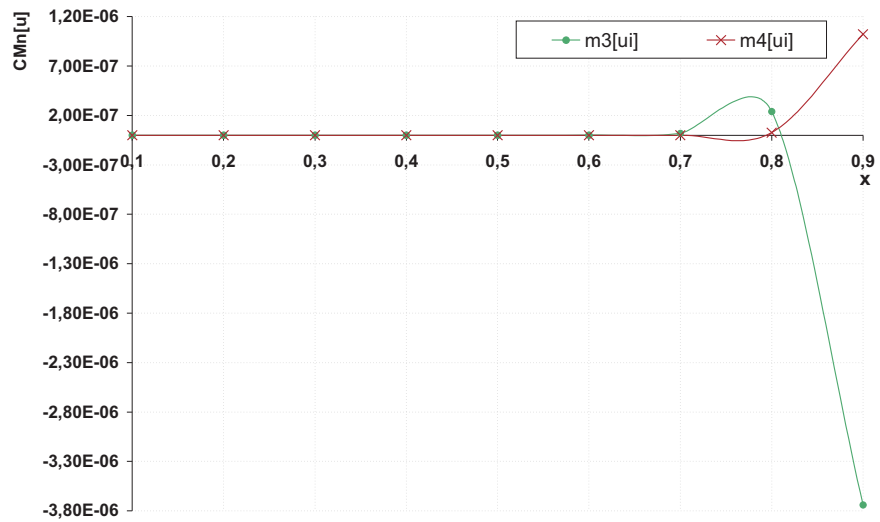


Figure 11 Higher moments of the fluid velocity as a function of the vertical coordinate

for CV_2 where

$$\sum_c F_c = \int_V q dV = 18 \quad (51)$$

for both CVs. Finally, after including the boundary conditions

$$\begin{aligned} T_P &= T_1 & \text{and} & & T_E &= T_2 & \text{for } CV_1 \\ T_P &= T_2 & \text{and} & & T_W &= T_1 & \text{for } CV_2 \end{aligned} \quad (52)$$

we obtain the linear system of equation, which is a start point to the perturbation analysis.

$$98T_1 - 17T_2 = 1386 \quad \text{and} \quad 98T_2 - 17T_1 = 1746 \quad (53)$$

The zeroth, first and second order conductivity matrices for a random heat conductivity for two CVs are defined as

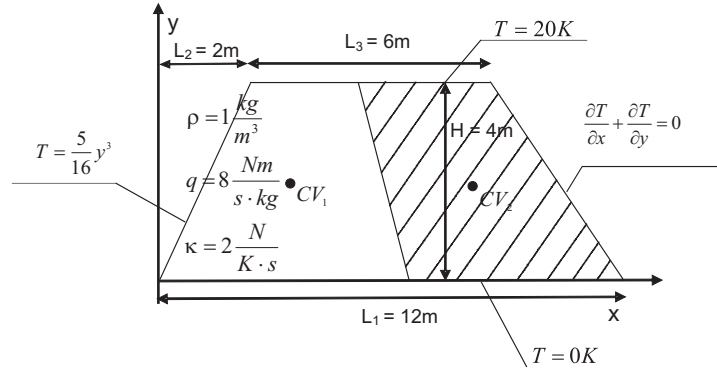


Figure 12 Boundary conditions and CV's definition for trapezoidal plate

$$\begin{aligned} \mathbf{K}_{2 \times 2}^0 &= -\frac{k}{2} \begin{bmatrix} 98 & -17 \\ -17 & 98 \end{bmatrix} \\ \mathbf{K}_{2 \times 2}^b &= -\frac{1}{2} \begin{bmatrix} 98 & -17 \\ -17 & 98 \end{bmatrix} \\ \mathbf{K}_{2 \times 2}^{bb} &= \begin{bmatrix} 0 & 0 \\ 0 & 0 \end{bmatrix} \text{ etc.} \end{aligned} \quad (54)$$

and the zeroth order vector of applied heat fluxes equals

$$\mathbf{Q}_2^0 = [1386 \quad 1746] \quad (55)$$

The final deterministic solution received in this case is obtained as

$$\mathbf{T}_2^0 = \left[\frac{2452}{69} \cdot \frac{1}{k} \quad \frac{2884}{69} \cdot \frac{1}{k} \right] \quad (56)$$

All numerical results of the stochastic analysis are presented on Tables 1 and 2 as well as in Figs 13–18. Table 1 presents the statistical estimators of the expectations and variances for the temperatures computed using the deterministic scheme of the Finite Volume Method in conjunction with the Monte–Carlo simulation routines for 10, 100, 1.000, 10.000 and 100.000 random samples. They are compared accordingly with the results of the response function approach embedded into the Stochastic perturbation-based Finite Volume Method, which is completed for the SFVM validation and to check the statistical convergence of basic discrete probabilistic characteristics.

It is clear from the comparison of both tables with each other that the statistical estimators for the increasing number of random trials tend to the result, which is very close to the limiting value taken from the perturbation theory of the systematically increased order. It is especially clear from the expectations, whereas higher order moments and statistics convergence need some more advanced computational studies. Nevertheless, we would like to prove numerically the hypothesis that the m^{th} central probabilistic moment shows the following tendency:

$$\lim_{N, n \rightarrow \infty} |\mu_m^n(u(b)) - \mu_m^N(u(b))| = 0 \quad (57)$$

Table 1 Statistical estimators of the expectations and variances for the temperatures

n	10^1	10^2	10^3	10^4	10^5
E[T ₁]	18,76338	18,61372	18,19293	18,25017	18,20043
Var[T ₁]	18,004	10,12188	8,017031	8,654043	8,700688
Var[T ₂]	24,90684	14,00266	11,09081	11,97205	12,03658

Table 2 Expected values and variances computed by response function perturbation-based method

n	2	4	6	8	10
E[T ₁]	18,1679	18,19505	18,19257	18,2098	18,21
E[T ₂]	21,36877	21,40043	21,40593	21,40288	21,40285
Var[T ₁]	7,103385	8,541564	8,832316		
Var[T ₂]	9,826865	11,81698	12,18186		

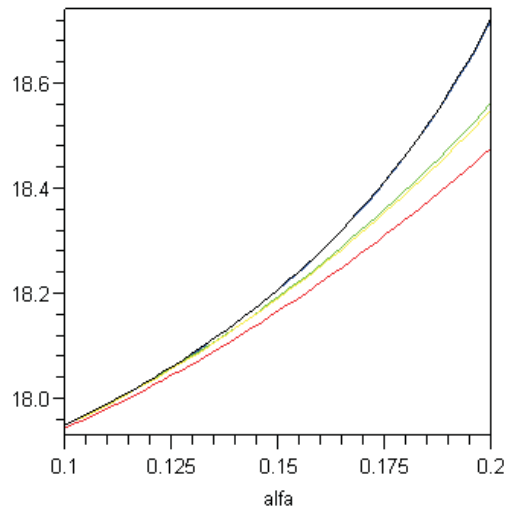


Figure 13 Expected values of the temperatures T_1 according to 2nd, 4th, 6th, 8th and 10th order theories

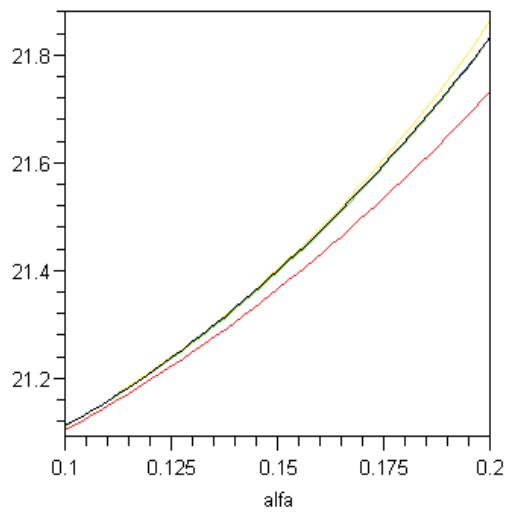


Figure 14 Expected values of the temperatures T_2 according to 2nd, 4th, 6th, 8th and 10th order theories

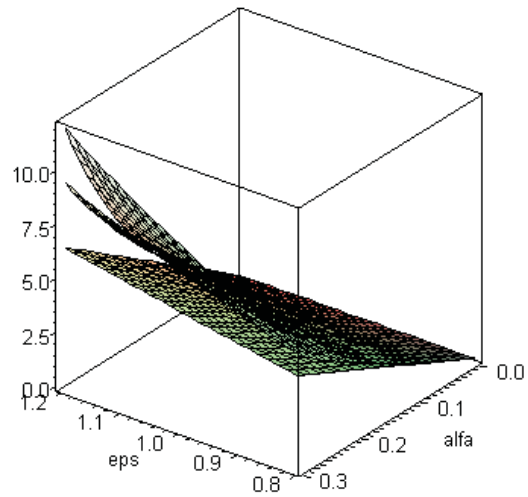


Figure 15 Standard deviations of the temperatures T_1 according to 2^{nd} , 4^{th} and 6^{th} order theories

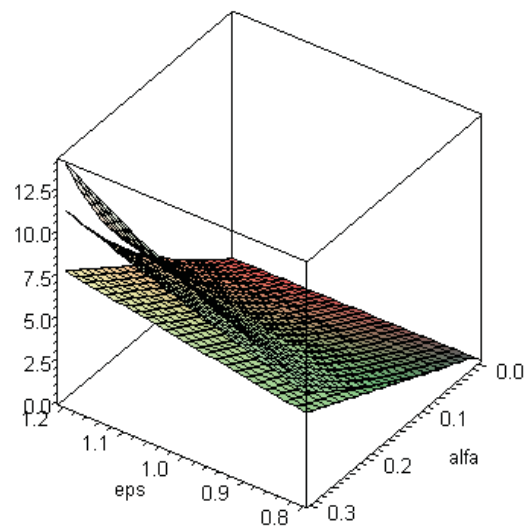


Figure 16 Standard deviations of the temperatures T_2 according to 2^{nd} , 4^{th} and 6^{th} order theories

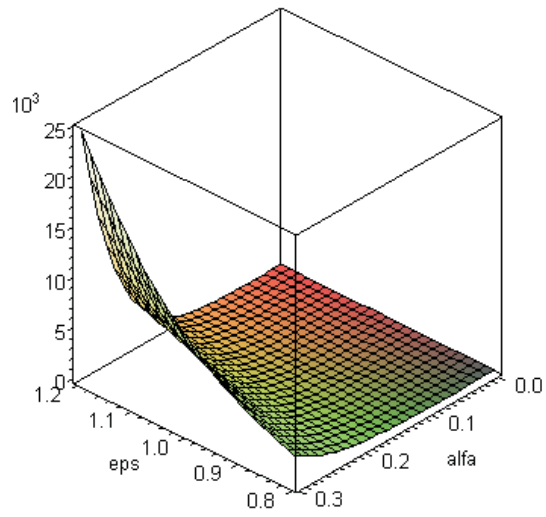


Figure 17 Fourth order central probabilistic moments for T_1 according to the lowest order theory

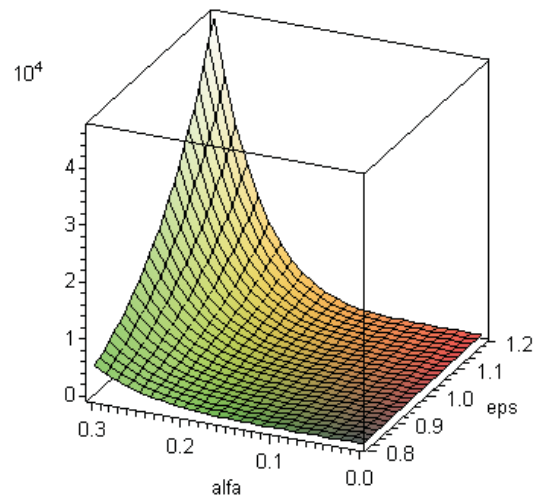


Figure 18 Fourth order central probabilistic moments for T_2 according to the lowest order theory

resulting from the perturbation theory $\mu_m^n(u(b))$ converges to its statistical estimator $\mu_m^N(u(b))$.

Next, the expected values of the temperatures T_1 and T_2 are computed and presented in Figs 13, 14, respectively, as the functions of the input coefficient of variation ranging from 0.0 for deterministic analysis to 0.2. Those computations are completed consistently with the 2nd, 4th, 6th, 8th and 10th order theories according to eqn (39); the green curve denotes each time an approximation of the highest order. Analogous comparison is done concerning the standard deviations of the temperature T_1 and T_2 (Figs 15 and 16), however now we have a new independent parameter – ε , but in this case we compare the 2nd, 4th and 6th order approximations only, considering a complex character for higher order formulas. Finally, Figs. 17 and 18 contain the fourth central moments of the previously observed temperatures, where the presentation idea as the surfaces with perturbation parameter and input coefficient of variation as the independent variables remains the same as before.

One may conclude from those results that the convergence of the SFVM in its generalized form is unquestionable for any values of the input coefficient of variation and may be corrected by an additional modification of the perturbation parameter ε . As it was expected, all the moments shown here are nonlinear functions of $\alpha(b)$ and even for a maximum value of this parameter, a difference between the neighboring perturbation order results decrease with an increase of the order n . Sometimes, like in the case of the expectations, this convergence has asymptotic behavior, where some higher orders bring the negative components and all probabilistic moments not necessarily increase for $n \rightarrow \infty$.

5. Concluding remarks

Mathematical derivations and computational implementation of the Stochastic Finite Volume Method for unidirectional and plane problems show that a probabilistic extension of the traditional deterministic Finite Volume Method towards random flows modeling is a relatively easy task. The computational studies demonstrate that the application of the generalized version of the stochastic perturbation technique returns almost the perfect agreement of the SFVM with the Monte–Carlo simulation built upon the deterministic FVM approach. The symbolic computational environment appeared to be a good numerical platform to perform all necessary computations presented here, like the similar studies contained in [6] neglecting whether the straightforward perturbations or the response function method are to be embedded. The future works on multivariable stochastic problems, the random processes perturbation-based modeling as well as coupling of various physical fields will make the Stochastic Finite Volume Method a very attractive and efficient computational tool.

Acknowledgments

The first author would like to acknowledge the financial support of the research grant from the Ministry of Research and Higher Education NN 519 386 636.

References

- [1] **Bijelonja, I., Demirdzic, I. and Muzaferija, S.:** A finite volume method for incompressible linear elasticity, *Computer Methods in Applied Mechanics and Engineering*, 195, 6378–6390, **2006**.
- [2] **Carslaw, H.S. and Jaeger, J.C.:** Conduction of Heat in Solids, Oxford Sci. Pub., Clarendon Press, Oxford, **1986**.
- [3] **Cueto–Felgueroso, L., Colominas, I., Nogueira, X. and Casteleiro, M.:** Finite volume solvers and Moving Least–Squares approximations for the compressible Navier–Stokes equations on unstructured grids, *Computer Methods in Applied Mechanics and Engineering*, 196, 4712–4736, **2007**.
- [4] **Durany, J., Pereira, J. and Varas, F.:** A cell–vertex finite volume method for thermohydrodynamic problems in lubrication theory, *Computer Methods in Applied Mechanics and Engineering*, 195, 5949–5961, **2006**.
- [5] **Ghanem, R.G. and Spanos, P.D.:** Stochastic Finite Elements. A Spectral Approach, *Dover Publ. Inc.*, New York, **2002**.
- [6] **Kamiński, M.:** On generalized stochastic perturbation–based finite element method, *Communications in Numerical Methods in Engineering*, **22**, 23–31, **2006**.
- [7] **Kamiński, M. and Ossowski, R.:** An introduction to the perturbation–based stochastic finite volume method for plane heat conduction problems, *Proceedings of the 12th WSEAS international conference on Computers*, p. 1032–1038, 23–25, Heraklion, Greece, **2008**.
- [8] **Kleiber, M. and Hien, T. D.:** The Stochastic Finite Element Method, Wiley, Chichester, **1992**.
- [9] **Schäfer, M.:** Computational Engineering – Introduction to Numerical Methods, *Springer Verlag*, Berlin, **2006**.
- [10] **Xiu, D.:** Efficient collocational approach for parametric uncertainty analysis, *Comm. Comput. Phys.*, 2, 2, 293–309, **2007**.

